Low-frequency properties of the phonon spectra, and low-temperature thermodynamics of disordered solid solutions

Cite as: Low Temp. Phys. **40**, 1013 (2014); https://doi.org/10.1063/1.4901989
Published Online: 03 December 2014

I. A. Gospodarev, V. I. Grishayev, A. V. Eremenko, M. S. Klochko, A. V. Kotlyar, E. V. Manzheliy, E. S. Syrkin, and S. B. Feodosyev

LATTICE DYNAMICS

Low-frequency properties of the phonon spectra, and low-temperature thermodynamics of disordered solid solutions

I. A. Gospodarev,[a] V. I. Grishayev, A. V. Eremenko, M. S. Klochko, A. V. Kotlyar, E. V. Manzheliy, E. S. Syrkin, and S. B. Feodosyev

B. Verkin Institute for Low Temperature Physics and Engineering, National Academy of Sciences of Ukraine, pr. Lenina 47, Kharkov 61103, Ukraine

(Submitted May 16, 2014; revised June 10, 2014)
Fiz. Nizk. Temp. **40**, 1296–1311 (November 2014)

This is an analysis of the properties of quasi-local vibrations, and the conditions of the formation thereof, in a realistic model of the crystal lattice on a microscopic scale. The evolution of quasi-local vibrations with an increase in the concentration of impurity atoms, is examined. It is shown that the formation of boson peaks occurs mainly due to the additional dispersion of high-velocity acoustic phonons (connected to the atomic vibrations of the main lattice), caused by the scattering of these phonons by the quasi-local vibrations localized at the impurities. We demonstrate a connection between the boson peaks in disordered systems, and the first van Hove singularity, in regular crystal structures. We analyze the manifestation of quasi-local vibrations and boson peaks, as it relates to the behavior of low-temperature heat capacity, and how it changes with an increasing impurity concentration. © *2014 AIP Publishing LLC*.
[http://dx.doi.org/10.1063/1.4901989]

1. Introduction

At low temperatures, vibrational thermodynamic characteristics of ordered and disordered systems, are determined mainly by the long-wave acoustic phonons, the dispersion law of which can be assumed to be linear. These phonons, regardless of polarization, distribute themselves freely along all crystallographic directions, similar to phonons in acoustic isotopic environments. Due to the discreteness of the crystal lattice, the phonon dispersion law deviates from the linear, as phonon frequency increases. Furthermore, an additional dispersion of phonons can occur due to the complexity of the crystal lattice, or the presence of defects. In these cases, little dispersions of quasi-localized states can occur within the phonon spectrum, which can scatter high-velocity acoustic phonons. Moreover, starting from a certain frequency ω^*, phonon dispersion of some polarizations and directions, stops. The frequency ω^* is called the propagon-diffusion border (PDB) frequency.[1] In Ref. 1 phonons with the frequency $\omega < \omega^*$ that are freely distributed in all crystallographic directions, are called *propagons*, whereas phonons with frequencies $\omega > \omega^*$, that cannot be distributed along certain directions, are *diffusions*.

In ideal crystals, the PDB frequency ω^*, matches the frequency of the first van Hove singularity, which corresponds to the isofrequency surface transition from closed to open, along some direction of quasi-momenta, $\mathbf{k}$, in space.[2] Of course, the understanding of the quasi-momentum and isofrequency surface, is applicable only to ordered systems, at the same time as the understanding of the propagon-diffusion border is also applicable to systems with a broken translational symmetry. The PDB manifests itself in the form of a distinct maximum along the ratio of the phonon density of states $\nu(\omega)$ to the square of frequency. This maximum, i.e., the abnormal excess of the phonon density of states in the low-frequency region above the Debye density of states, is referred to as the boson peak (BP) throughout literature.[3–7] Such maxima were observed in Raman and Brillouin scattering spectra,[8,9] and also in inelastic neutron scattering experiments.[10] They are manifested in the low-frequency region of the vibrational density of states, in the frequency range between 0.5 and 2 THz,[7,11,12] i.e., far below the Debye frequency. In Refs. 13–15 it is shown that the BP in disordered structures form in the frequency interval where the length of the phonon wave becomes comparable to the parameters of disorder, particularly with the average distance between defects (Ioffe-Regel limit). The boson peaks form distinctly on the temperature dependences of low-temperature heat capacity, as sharp maxima along the ratio of the heat capacity to the cube of the temperature (for example, see Ref. 16).

For crystals with a simple and highly symmetrical lattice, the dispersion law of low-frequency phonons, i.e., phonons with frequencies below the first van Hove singularity, is close to the dispersion law of sound $\omega_i(\mathbf{k}) \approx s_i(\boldsymbol{\kappa})k$, ($\boldsymbol{\kappa} \equiv \mathbf{k}/k$) and the vibrational properties of the ideal systems can be sufficiently well described within the framework of the Debye approximation. In the region of low frequencies the phonon density of states is the same as the Debye density of states, and therefore at $\omega \to 0$, the function $\nu(\omega) \sim \omega^2$ and its values, are small. As such, the introduction of defects into the crystal can significantly enrich the low-frequency region of the phonon spectrum, and lead not only to quantitative, but also to qualitative changes in the behavior of low-temperature vibrational properties.

Quasi-local vibrations (QLV) are the most studied low-frequency property of a phonon spectrum of a crystal, containing a point defect. QLV are sharp resonant

low-frequency peaks along the phonon density of states, theoretically predicted[17] and experimentally found,[18] in the middle of the last century. However, further analysis at the microscopic level of their properties, and the conditions under which they are formed, in addition to the QLV transformation during the increase in the concentration of impurity atoms, is still inadequately studied. It is this analysis in particular that allows us to examine the BP nature, and to describe all low-frequency properties of the phonon spectra of real crystals and solid solutions, from one point of view. It should be noted that the analysis must be done without directly calculating the quasi-wave vector, the introduction of which into the examined systems with significantly impaired crystal regularity of atom arrangement, always requires additional substantiation, is artificial, and not always correct.

For our calculations, we will use the method of Jacobi matrices,[19–22] which does not use the crystal translational symmetry in an explicit way, and allows for the calculation of the local Green functions and local spectral densities, without calculating dispersion laws and involving the quasi-wave vectors. These functions are self-averaging quantities.[23,24] The description of the vibrational spectrum of a disordered solid solution using the given spectral properties is more correct, especially since the natural form of describing the localized or quasi-localized states, is their expansion along the moments, which coincides practically with the classification of vibrations, adopted in the method of Jacobi matrices (*J*-matrices). The basis for this method, in a volume that is appropriate for reading this article, is presented in Section 2.

The third section is dedicated to the analysis of the QLV properties and the conditions for the formation thereof, at the microscopic level. The evolution of the QLV is studied, with an increase in the concentration of impurity atoms.

In the fourth section, on a realistic model of the crystal lattice, it is shown that the formation of boson peaks is caused by additional dispersion of high-velocity acoustic phonons, caused by the scattering of these phonons (connected to the vibrations of the atoms of the main lattice) by QLV, localized around the impurities. We analyze the similarity between BP in disordered systems, and the first van Hove singularity in regular crystal structures.

The fifth section is dedicated to the analysis of the manifestation of quasi-local vibrations and boson peaks, in the behavior of low-temperature heat capacity with an increase in the concentration of impurities.

2. Fundamentals of the method of Jacobi matrices

We will write down the equation for the harmonic vibration of the crystal lattice in the operator form

$$(\hat{L} - \omega^2 \hat{I})\vec{\psi} = 0, \tag{1}$$

where ω is the natural vibration frequency; $\hat{I}$ is the unit operator, and operator

$$\hat{L} = \hat{L}(\mathbf{r}, \mathbf{r}') \equiv \frac{\hat{\Phi}(\mathbf{r}, \mathbf{r}')}{\sqrt{m(\mathbf{r})m(\mathbf{r}')}}$$

describes the harmonic vibrations of the crystal ($\hat{\Phi}(\mathbf{r}, \mathbf{r}')$ is the matrix of the force constants, corresponding to the interaction of atoms with the radius vectors $\mathbf{r}$ and $\mathbf{r}'$, whereas $m(\mathbf{r})$ and $m(\mathbf{r}')$ are the masses of these atoms). The $\hat{L}$ operator works in a $3N$-dimensional ($N \to \infty$ is the number of atoms in the crystal) space of atomic displacements H, the vectors of which, $\vec{\psi}$ are designated with an arrow above the symbol throughout this article (as opposed to usual three-dimensional vectors, which are conventionally denoted in bold font).

Having selected a certain vector $\vec{h}_0 \in H$ in space H, corresponding to some displacement of a certain atom or group of atoms (so-called *generating vector*), we can build the sequence $\{\hat{L}^n \vec{h}_0\}_{n=0}^{\infty}$. The linear hull of the sequence of these vectors, forms the subspace $H^{(i)} \subset H$ invariant relative to operator's $\hat{L}$ *cyclic subspace*. In the basis $\{\vec{h}_n\}_{n=0}^{\infty}$, derived by the orthonormalization of the sequence $\{\hat{L}^n \vec{h}_0\}_{n=0}^{\infty}$, the operator $\hat{L}^{(i)}$, induced by operator $\hat{L}$ in subspace $H^{(i)}$, has a nondegenerate spectrum and is presented in the basis $\{\vec{h}_n\}_{n=0}^{\infty}$ as a tridiagonal (Jacobi) matrix

$$L_{mn}^{(i)} = a_n^{(i)} \delta_{mn} + b_n^{(i)} (\delta_{m,n+1} + \delta_{m+1,n}).$$

In the same basis, the matrix elements of the Green operator $\hat{G}(\omega^2) = (\omega^2 \hat{I} - \hat{L})^{-1}$ look like

$$G_{mn}^{(i)}(\omega^2) = -P_m^{(i)}(\omega^2) Q_n^{(i)}(\omega^2) + P_m^{(i)}(\omega^2) P_n^{(i)}(\omega^2) G^{(i)}(\omega^2). \tag{2}$$

In (2) the function

$$G^{(i)}(\omega^2) \equiv G_{00}^{(i)}(\omega^2) = (\vec{h}_0^{(i)}, \hat{G}^{(i)}(\omega^2) \vec{h}_0^{(i)})$$

is the *local Green function*, which corresponds to a displacement of one or several atoms* defined by the generating vector $\vec{h}_0^{(i)}$, and $P_m(x)$ are polynomials that are defined by the recurrence relation

$$b_m P_{m+1}(x) = (x - a_m) P_m(x) - b_{m-1} P_{m-1}(x), \tag{3}$$

with the initial conditions: $P_{-1}(x) \equiv 0$; $P_0(x) \equiv 1$, and polynomials $Q_m(x)$ are defined by the same recurrent expression, but with the initial conditions $Q_0(x) \equiv 0$; $Q_1(x) \equiv {b_0}^{-1}$. Up to the normalization factor $\prod_{i=0}^{n-1} b_i^{-1}$, the polynomial $P_m(\omega^2)$ coincides with the determinant of the matrix $|\omega^2 \delta_{ik} - L_{ik}|_{i,k=0}^{m}$, whereas polynomials $Q_m(\omega^2)$ coincide with the minor of the first diagonal element of this determinant. From the construction of the $\{\vec{h}_n\}_{n=0}^{\infty}$ basis, and the recurrence relation (3) we get

$$\vec{h}_n = P_n(\hat{L}) \vec{h}_0. \tag{4}$$

The eigenfunction $\vec{\psi}(\omega^2)$ corresponding to the eigenvalue $\lambda \equiv \omega^2$, looks like

$$\vec{\psi}(\omega^2) = \sum_n P_n(\omega^2) \vec{h}_n. \tag{5}$$

If the band of the continuous spectrum is connected to $\omega \in [0, \omega_m]$, then the matrix elements of the *J*-matrix, approach the following limits as the rank increases:

*Subsequently, the index that numbers the cyclic subspaces will only be written when it is necessary to differentiate one subspace from another.

$$\lim_{n\to\infty} a_n = 2\lim_{n\to\infty} b_n = \frac{\omega_m^2}{2}. \quad (6)$$

In practice, it is usually possible to calculate a finite number for the J-matrix elements of the $\hat{L}$ operator (for example, before a_n and b_{n-1}, inclusive)then, setting the rest of the matrix elements equal to their limit values (6), we can write the local Green function $G(\omega^2)$ as a *continued fraction*, that folds into the following expression:

$$G(\omega^2) \equiv G_{00}(\omega^2) = \frac{Q_n(\omega^2) - b_{n-1}Q_{n-1}(\omega^2)K_\infty(\omega^2)}{P_n(\omega^2) - b_{n-1}P_{n-1}(\omega^2)K_\infty(\omega^2)}, \quad (7)$$

where $K_\infty(\omega^2)$ is the continued fraction, corresponding to the J-matrix, all elements of which are equal to the limit values (6)

$$K_\infty(\omega^2) = \frac{4}{\omega_m^4}\left[2\omega^2 - \omega_m^2 + 2Z(\omega)\sqrt{|\omega^2(\omega^2-\omega_m^2)|}\right], \quad (8)$$

where

$$Z(\omega) = i\Theta(\omega)\Theta(\omega_m - \omega) - \Theta(\omega - \omega_m). \quad (9)$$

The value

$$\rho^{(\vec{h}_0)}(\omega) \equiv 2\omega\rho^{(\vec{h}_0)}(\omega^2) = \frac{2\omega}{\pi}\lim_{\gamma\to+0}\operatorname{Im} G^{(\vec{h}_0)}(\omega^2 + i\gamma) \quad (10)$$

is referred to as the *spectral density* generated by the $\vec{h}_0$ vector, whereas the phonon density of states in the cyclic subspace generated by the vector $\vec{h}_0$, i.e., the value

$$\nu^{(\vec{h}_0)}(\omega) \equiv 2\omega g^{(\vec{h}_0)}(\omega^2) = \frac{2\omega}{\pi}\lim_{\gamma\to+0}\operatorname{Im}\operatorname{Sp}\hat{G}^{(\vec{h}_0)}(\omega^2 + i\gamma),$$

in accordance to (2), can be written as

$$\begin{aligned}\nu^{(\vec{h}_0)}(\omega) &\equiv 2\omega g^{(\vec{h}_0)}(\omega^2)\\ &= \rho^{(\vec{h}_0)}(\omega)\lim_{N\to\infty}\sum_{n=0}^{3N}P_n^2(\omega^2)\\ &= 2\omega\rho^{(\vec{h}_0)}(\omega^2)\lim_{N\to\infty}\sum_{n=0}^{3N}P_n^2(\omega^2)\end{aligned} \quad (11)$$

(all phonon density of states and spectral densities are normalized by one). As follows from expressions (7)–(9), in expression (10) it is possible to go directly to the limit at $\gamma \to 0$, and, introducing Green's function $G(\omega) = 2\omega G(\omega^2)$, for spectral densities (10) and density of states (11) write down:

$$\begin{aligned}\rho^{(\vec{h}_0)}(\omega) &= \frac{1}{\pi}\operatorname{Im}\hat{G}^{(\vec{h}_0)}(\omega);\\ \nu^{(\vec{h}_0)}(\omega) &= \rho^{(\vec{h}_0)}(\omega)\lim_{N\to\infty}\sum_{n=0}^{3N}P_n^2(\omega^2).\end{aligned} \quad (12)$$

From another side, from the procedure of building the cyclic subspaces, it follows that the total phonon density of states of the crystal, is equal to the arithmetic mean of spectral densities, generated by all linearly independent displacements.

The Jacobi method does not make explicit use of the translational symmetry of the lattice, but for an ideal crystal, the unit cell of which contains q atoms, it is conveniently written as

$$\nu(\omega) = \frac{1}{3q}\sum_{s=1}^{q}\sum_{i=1}^{3}\rho_i^{(s)}(\omega), \quad (13)$$

where $\rho_i^{(s)}(\omega)$ is the spectral density, generated by the displacement of an atom from the sublattice s, along the crystallographic direction i.

3. Quasi-local vibrations, their formation, and evolution, with increasing concentration of impurity atoms

Quasi-local vibrations (for example, see Refs. 17, 25, and 26) are more commonly referred to as sharp resonance maxima, occurring in the low-frequency region of the phonon spectrum of the crystal, usually under the influence of small concentrations of defects, leading to an increase in the number of low-frequency phonons, for example, impurities that are heavy or loosely coupled to the atoms of the main lattice. At small concentrations of impurity atoms $p \ll 1$, the vibrational characteristics of the solid solution can be described using an expression for the density of states of the crystal with defects, in a linear p approximation, using J-matrices

$$\tilde{\nu}(\omega) \approx \nu(\omega) + p\sum_i \Delta\rho^{(i)}(\omega). \quad (14)$$

The summation in (14) is over all cyclic subspaces, in which the operator $\hat{\Lambda}$, describing the perturbation of the lattice vibrations of an isolated heavy, or loosely coupled substitutional impurity, is other than zero; $\Delta\rho^{(i)}(\omega)$ is the change of the spectral density in each of such subspaces; $\tilde{\nu}(\omega)$ and $\nu(\omega)$ are the phonon density of states of the solid solution and the ideal crystal, respectively.

If in a cyclic subspace $H^{(i)}$ the operator $\hat{\Lambda}$ induces a regular degenerate operator,[27,28] the value $\Delta\rho^{(i)}(\omega)$ can be calculated using the spectral shift function. Using the expressions derived for this function via the J-matrix method,[19,20] we get

$$\begin{aligned}\Delta\rho^{(i)}(\omega) &= -\frac{d\xi^{(i)}(\omega)}{d\omega}\\ &= \frac{[\rho^{(i)}(\omega)]^2}{[\pi\rho^{(i)}(\omega)]^2 + [S^{(i)}(\omega) - \operatorname{Re} G^{(i)}(\omega)]^2}\\ &\quad\times\frac{d}{d\omega}\left[\frac{S^{(i)}(\omega) - \operatorname{Re} G^{(i)}(\omega)}{\rho^{(i)}(\omega)}\right].\end{aligned} \quad (15)$$

In (15), the value $\xi^{(i)}(\omega)$ is the spectral shift function in the cyclic subspace $H^{(i)}$; the function $S^{(i)}(\omega)$ describes the defect-induced perturbation, and depends on the defect parameters, $G^{(i)}(\omega)$ is the local Green function for the ideal crystal. If in any cyclic subspace (indexes labeling the subspaces will be omitted later) the equation

$$S(\omega) - \operatorname{Re} G(\omega) = 0 \quad (16)$$

has the solution $\omega = \omega_k$, then in the vicinity of this point, the frequency dependence (15) obtains a resonance form

$$-\frac{d\xi(\omega)}{d\omega} = \frac{2}{\pi}\frac{\Gamma}{4(\omega-\omega_k)^2+\Gamma^2};$$
$$\Gamma \equiv \frac{\pi\rho(\omega)}{\dfrac{d}{d\omega}[S(\omega)-\operatorname{Re}G(\omega)]_{\omega=\omega_k}}. \qquad (17)$$

This resonance maximum along the phonon density of states of the crystal with defects, got the name *quasi-local vibrations (QLV)*.

We will note that Eq. (16) formally matches the Lifshitz equation, which determines (of course, for other defect parameters, and therefore, other values of the $S(\omega)$ function), the frequencies of discrete vibrational levels, lying outside the band of the quasi-continuous spectrum of the crystal.[27,28] However, the given discrete levels, in contrast to the values of ω_k, are the poles of the perturbed local Green function, but Green functions cannot have poles within the band of the quasi-continuous spectrum, which follows, for example, from (2) and (7)–(9). The possibility of determining the QLV frequencies using Eq. (3) exists due to the fact that at low frequencies, $\operatorname{Re}G(\omega) \gg \operatorname{Im}G(\omega)$, even though for many real values for the parameters of the defect at $\omega = \omega_k$, the value of the spectral density of an ideal crystal cannot be considered as being negligibly small.

We will analyze the QLV occurring due to the substitutional impurity, in a FCC crystal with central interaction with its nearest neighbors

$$\Phi_{ik}(\Delta) = \frac{\omega_m^2}{8}\frac{\Delta_i\Delta_k}{\Delta^2}$$

($\Delta \equiv \mathbf{r}-\mathbf{r}'$ is the difference between the radius vectors of the interacting atoms). The interaction of the impurity with the main lattice will also be considered as being strictly central, and therefore any displacement it causes will be regular and degenerating. We will examine two cases: the isotopic impurity with mass four times bigger than the mass of the main lattice (i.e., the mass of the defect is $\varepsilon \equiv \Delta m/m = 3$ where m is the mass of the main lattice), and also an impurity atom with a mass equal to the mass of the atom in the main lattice ($\varepsilon = 0$) but with a coupling to the main lattice that is four times weaker than the coupling main lattice atoms have amongst themselves (coupling defect, written as $\upsilon = \Delta\alpha/\alpha = -3/4$, where $\alpha = m\omega_m^2/8$, is the force constant describing the interaction of the atoms of the main lattice). In the first case, the $\hat{\Lambda}$ operator induces the nonzero operator only in the cyclic subspace, generated by the displacement of the impurity atom. The vectors belonging to this subspace transform according to the irreducible representation τ_-^5 of the symmetry group of the examined lattice O_h (designation from Ref. 29). In the given subspace, the spectral density of the ideal lattice coincides with its density of states. The function $S(\omega,\varepsilon)$ for an isotopic impurity looks like [19,20]

$$S(\omega) = -\frac{2}{\omega\varepsilon}. \qquad (18)$$

A solution for Eq. (16) for the given case, is presented in Fig. 1(a).

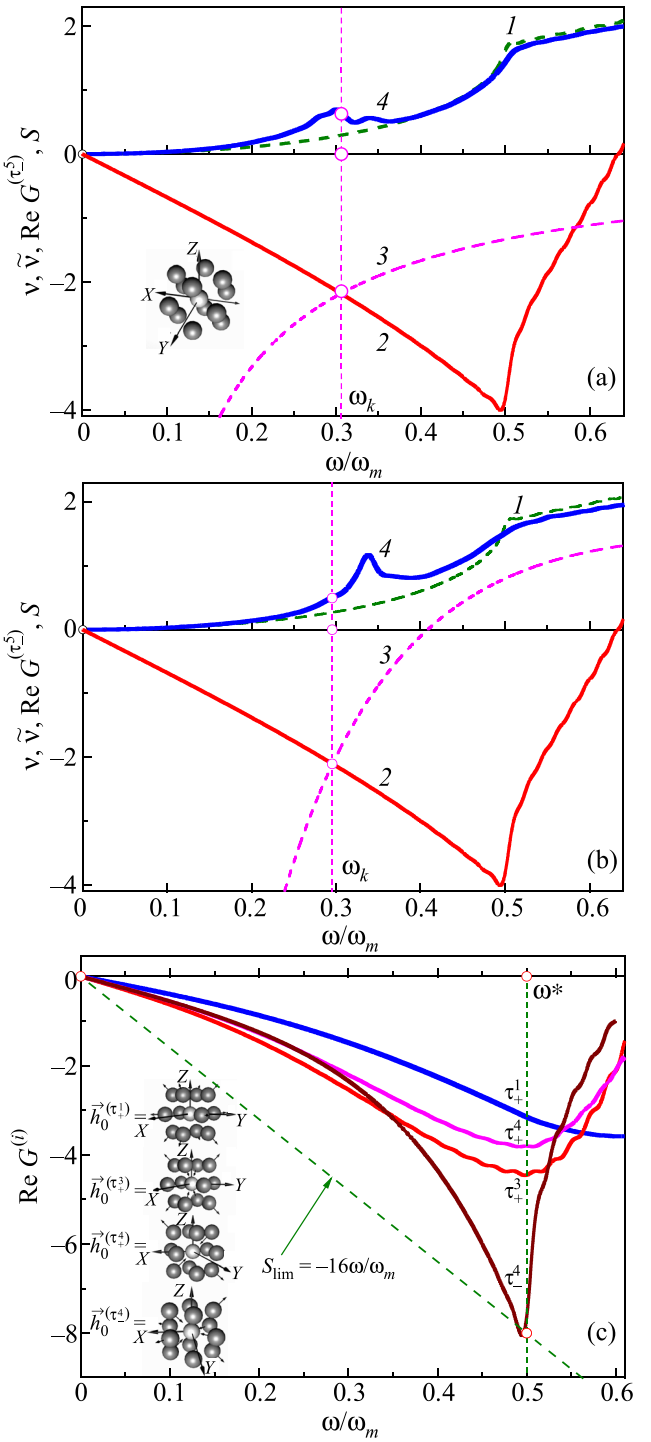

FIG. 1. Real parts of the Green function and a solution of the Lifshitz equation in different cyclic subspaces: heavy isotopic impurity (a), loosely coupled impurity (b), (c).

In the second case, except for the subspace $H^{(\tau_-^5)}$, in which the function $S(\omega,\upsilon)$, looks like

$$S_w^{(\tau_-^5)}(\omega,\upsilon) = \frac{2}{\omega} + \frac{\omega_m^2}{\omega^3}\frac{1+\upsilon}{\upsilon}, \qquad (19)$$

and solutions for Eq. (16) are presented in Fig. 1(b), the non-zero operators will be those induced by the $\hat{\Lambda}$ operator in the cyclic subspaces, transformed according to irreducible representations τ_+^1, τ_+^3, τ_+^4, and τ_-^4 of the same group, O_h. In all four of these subspaces, the functions $S(\omega,\upsilon)$ coincide with

$$S_w^{(\tau_+^1)}(\omega,\upsilon) = S_w^{(\tau_+^3)}(\omega,\upsilon) = S_w^{(\tau_+^4)}(\omega,\upsilon) = S_w^{(\tau_-^4)}(\omega,\upsilon)$$
$$\equiv S'_w(\omega,\upsilon) = \frac{16\omega}{\omega_m^2\upsilon}.$$

Fig. 1(c) shows generating vectors of the given subspaces, and frequency dependences of the real parts of the Green functions in each of them. For loosely coupled impurities ($\upsilon < 0$) the function $S'_w(\omega,\upsilon) \le S_{\lim} = -16\omega/\omega_m^2$, and, as seen in Fig. 1(c), Eq. (16), cannot have solutions in the cyclic subspaces $H^{(\tau_+^1)}$, $H^{(\tau_+^3)}$, and $H^{(\tau_+^4)}$.

In subspace $H^{(\tau_-^4)}$, a solution is possible for the impurity, the force interaction of which, with the atoms of the main lattice, is at least 50 times weaker than the interaction of the atoms of the main lattice between themselves, and at this value, ω_k will practically coincide with the first van Hove singularity (the frequency of this singularity will be labeled as ω^*). Therefore, in the case of a loosely coupled impurity, for real values of the υ parameter, Eq. (16) can have a solution only in subspace $H^{(\tau_-^5)}$.

In Figs. 1(a) and 1(b), the real part of the Green function (curves 2 in both panels) crosses the dashed curves 3, which represent the dependences in (18)—panel (a), and (19)—panel (b), at points ω_k. This same figure shows the spectral densities $\rho^{(\tau_-^5)}(\omega)$ of an ideal crystal, which coincide with its phonon density of states $\nu(\omega)$, shown in curves 1 (shaded), and also the phonon density of states of the corresponding solid solutions at concentrations $p = 5\%$, in curves 4.

At $\omega = \omega_k$, the value of the phonon density of states cannot be considered negligibly small ($\nu(\omega_k) \sim 0.1\ \mathrm{Re}\, G(\omega_k)$). Therefore, as seen in Figs. 1(a) and 1(b), that even though frequencies of the maxima on curves 4 are located in proximity to frequency ω_k, they do not coincide (especially in the case of a loosely coupled impurity, as shown in panel (b)). Also, for a loosely coupled impurity, a higher degree of QLV localization on impurity atoms is likely. Fig. 2 shows the local spectral densities of the impurity atoms and their closest neighbors, and also the spectral correlators of displacements of the impurity, with their first coordination sphere. In the figure, curves 1 are the phonon density of states of the ideal lattice; curves 2 are local spectral density of the impurity atoms

$$\tilde\rho^{(\tau_-^5)}(\omega) = \frac{2\omega}{\pi}\mathrm{Im}(\vec h_0^{(\tau_-^5)}, [\omega^2\hat I - \hat L - \hat\Lambda]^{-1}\vec h_0^{(\tau_-^5)}). \qquad (20)$$

The data of the dependence has a characteristic Lorentzian resonance, similar to (16), and contain no van Hove singularities. The frequencies of the maxima on these spectral densities (points ω_{ql}) differ from the frequency ω_k. Curves 3 and 4 in Fig. 2 are the spectral correlators of impurity atom displacements, with their first coordination sphere

$$\tilde\rho_{01}^{(\tau_-^5)}(\omega) = \frac{2\omega}{\pi}\mathrm{Im}(\vec h_1^{(\tau_-^5)}, [\omega^2\hat I - \hat L - \hat\Lambda]^{-1}\vec h_0^{(\tau_-^5)})$$
$$= P_1^{(\tau_-^5)}(\omega^2)\tilde\rho^{(\tau_-^5)}(\omega), \qquad (21)$$

and the values

$$\tilde\rho_{11}^{(\tau_-^5)}(\omega) = \frac{2\omega}{\pi}\mathrm{Im}(\vec h_1^{(\tau_-^5)}, [\omega^2\hat I - \hat L - \hat\Lambda]^{-1}\vec h_1^{(\tau_-^5)})$$
$$= [P_1^{(\tau_-^5)}(\omega^2)]^2\tilde\rho^{(\tau_-^5)}(\omega), \qquad (22)$$

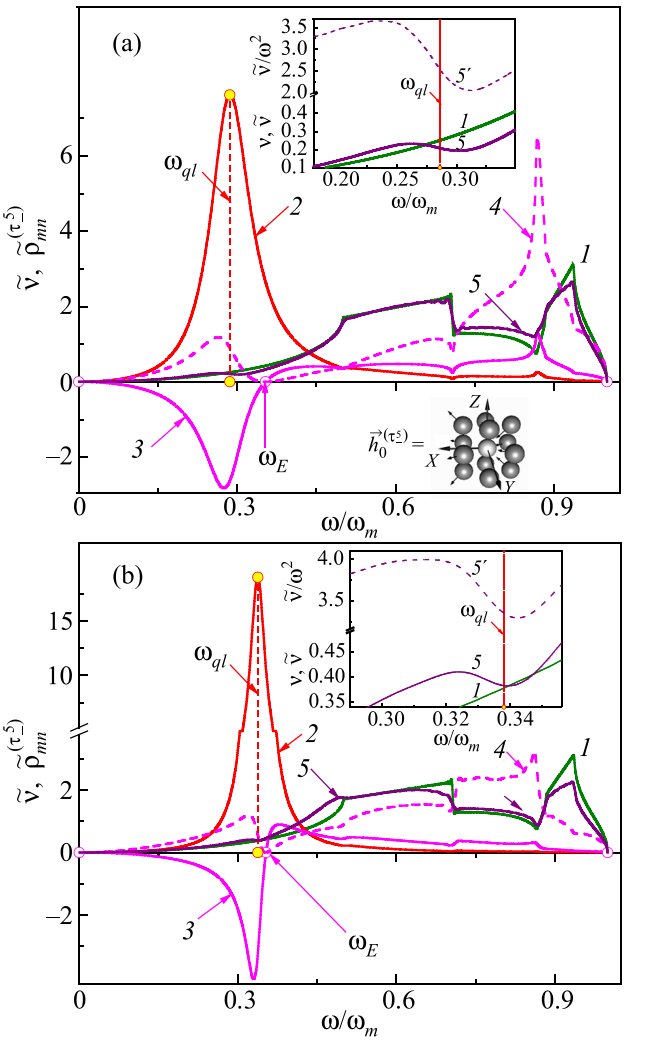

FIG. 2. The spectral density of the impurity, and its nearest neighboring atom: heavy isotopic impurity (a), loosely coupled impurity (b).

characterizing the input of cyclic subspaces, in which the QLV were formed, into the local spectral density of the closest neighbor of the impurity (curves 5). In (21) and (22), $\tilde P_1^{(\tau_-^5)}(\omega^2)$ are polynomials defined by expressions (3) for the J-matrix of the perturbed operator $\hat L + \hat\Lambda$ in the cyclic subspace $H^{(\tau_-^5)}$. These polynomials vanish at $\omega = \omega_E$, which is the instein frequency of the given subspace

$$\omega_E^2 = \int_0^{\omega_m}\omega^2\nu(\omega)d\omega \equiv a_0^{(\tau_-^5)}.$$

Therefore, at $\omega = \omega_E$, as follows from (3), the correlation with the first coordination sphere is absent, and the closer ω_{ql} gets to ω_E, the higher the degree of QLV localization. It can be seen that the ω_{ql} frequency for loosely coupled impurities, is approximately three times closer to ω_E, than for isotopic impurity, and the quasi-local maximum has a sharper resonance for loosely coupled impurities, than for a heavy isotope.

The vanishing of the $\tilde\rho_{01}^{(\tau_-^5)}(\omega_E)$ and $\tilde\rho_{11}^{(\tau_-^5)}(\omega_E)$ values is due to the non-monotonic behavior (i.e., significant deviation from Debye type) of curves 5 within the proximity of the frequency ω_{ql}. Such "Non-Debye" behavior on the phonon spectrum of the closest impurity neighbor, is more noticeable

in the ratio of these local spectral densities to the square of the frequency (curve 5' on the magnified panels of both parts of the figure).

Fig. 3 shows the phonon density of states of disordered solid solutions, formed by the introduction of ($p = 5\%$) heavy (Fig. 3(a)) and loosely coupled (Fig. 3(b)) impurity atoms $\tilde{\nu}(\omega)$. Curves 2 on both panels are inputs into the given values from the vibrations of impurity atoms $\nu_{\text{imp}}(\omega)$; curves 3 are atoms of the main lattice $\tilde{\nu}(\omega) - \nu_{\text{imp}}(\omega)$, and curves 4 (curves 1 are the phonon density of states of the ideal lattice) are compared with the local spectral densities of the isolated impurity; curves 5 represent the value of $p\tilde{\rho}^{(\tau^5)}(\omega)$ and its closest neighbors; curves 6 are $(1-p)\tilde{\nu}_{1n}(\omega)$. The maximums on curves 3 and 5 coincide with sufficient precision, especially in the case of loosely coupled impurities. This serves as evidence of strong QLV localization on the impurity atoms. Therefore, the frequency ω_{ql} can be defined as *quasi-local*, with more justification than ω_k. Within the proximity of this frequency, curves 4 and 6 experience similar fractures (at $p = 5\%$ the majority of the atoms of the main lattice of the solution have an impurity atom among its closest neighbors). Therefore, in close proximity to the quasi-local frequency ω_{ql}, the local spectral

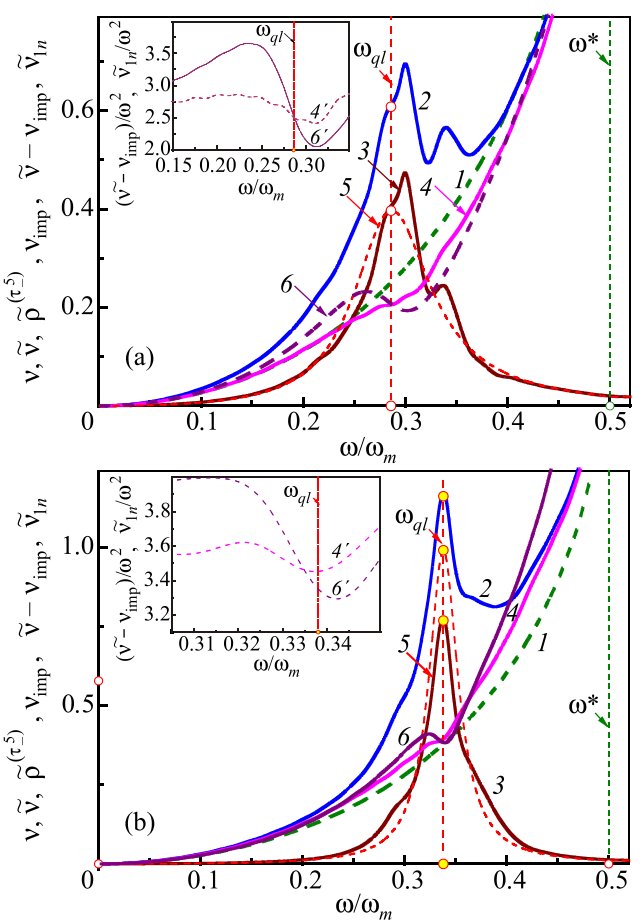

FIG. 3. Comparison of the phonon density of 5% solid solutions (2) and inputs into its system from vibrations of impurity atoms (3) and atoms of the main lattice (4) with spectral densities of the isolated impurity atom (5) and local spectral densities of the nearest neighbor of the impurity (6). Curves 1 are the phonon density of states of the ideal lattice. The magnified panels show the relationship of the contributions to the phonon density of solutions from the main lattice atoms (4'), and local spectral densities of the nearest neighbors of the isolated impurities (6'), to the square of the frequency. A heavy isotropic impurity (a), and a loosely coupled impurity (b).

densities of both the impurity atoms, and the atoms of the main lattice, lose their characteristic Debye form, which is noticeably demonstrated by curves 4' and 6' in the magnified panels, showing the relationships of the corresponding spectral densities (curves 4 and 6) to the square of the frequency.

Fig. 4 shows the evolution of the phonon density of states of the disordered solid solutions, with an increase in the concentration of heavy isotopic impurity. The figure shows phonon density of states $\tilde{\nu}(\omega,p)$ for concentrations $p = 0.05$, 0.10, 0.25, and 0.5 (solid lines on the corresponding panels of the figure). Along with these curves on each of the panels, as a reference, we see $\nu(\omega)$ dependences of the ideal crystal-matrix and also of the ideal lattice, composed of heavy $\varepsilon = 3$ atoms, which, in the description of the solution, are considered to be isotope-defects (thin dashed lines). The spectral density of the system $\rho(\omega)$, as a self-averaging value (for example, see Refs. 23 and 24), can be derived by the averaging of **r** across all positions, and directions of the displacements i, of the $\rho_i(\omega,\mathbf{r})$ function, which represents the spectral densities of cyclic subspaces, generated by atomic displacement with the radius-vector **r**, in the crystallographic direction i. We calculated the spectral densities $\tilde{\nu}(\omega,p) \equiv \langle\tilde{\rho}_i(\omega,\mathbf{r})\rangle_p$ for different concentrations of the randomly arranged impurity atoms. For each value of the concentration, the averaging was done for several thousand random configurations of impurity distributions, and for each configuration, the density of states was defined by the averaging of several tens of spectral densities, corresponding to the displacements along different crystallographic directions of a few tens of consecutively arranged atoms.

We will note right away, that by $p = 0.05$, the crystallographic regularity of the atomic arrangement was sufficiently impaired, and in describing the quasi-particle spectra of such a solution it is no longer possible to use the understanding of "*the first Brillouin zone*." At the same time, the function $\tilde{\nu}(\omega,p)$ in proximity of the frequency ω^*, qualitatively changes its behavior not only when $p = 0.05$, but also at $p = 0.1$, but this change is fully analogous to the changes in the behavior of the phonon density of states of the ideal crystal, in proximity to the first van Hove singularity. We will also remind you that the first van Hove singularity (for example, see Refs. 25 and 26) corresponds to the changes in topology of isofrequency surfaces, i.e., to a transition from a closed surface (at $\omega < \omega^*$) to open, along a certain direction in reciprocal space (at $\omega > \omega^*$). Such a transition occurs due to contact of the isofrequency surface with the boundary of the first Brillouin zone, and in the absence of a crystal translational symmetry, we cannot discuss it.

In the following section, the connection between the group velocities of the acoustic phonon modes, and the van Hove singularities, will be analyzed in more detail. Here we will note that the localization of phonons with certain polarization along some directions, occurring at specific frequencies, is not directly related to crystal translational symmetry, but will be inherent for disordered systems. In the case of an ideal crystal, the frequencies at which the "braking" of the next phonon mode occurs, are the same for the entire sample, and manifest themselves in the phonon density behavior as singularities, the form of which is determined by the lattice dimensions. For a structure with broken translational symmetry, each "braking" occurs within a certain frequency

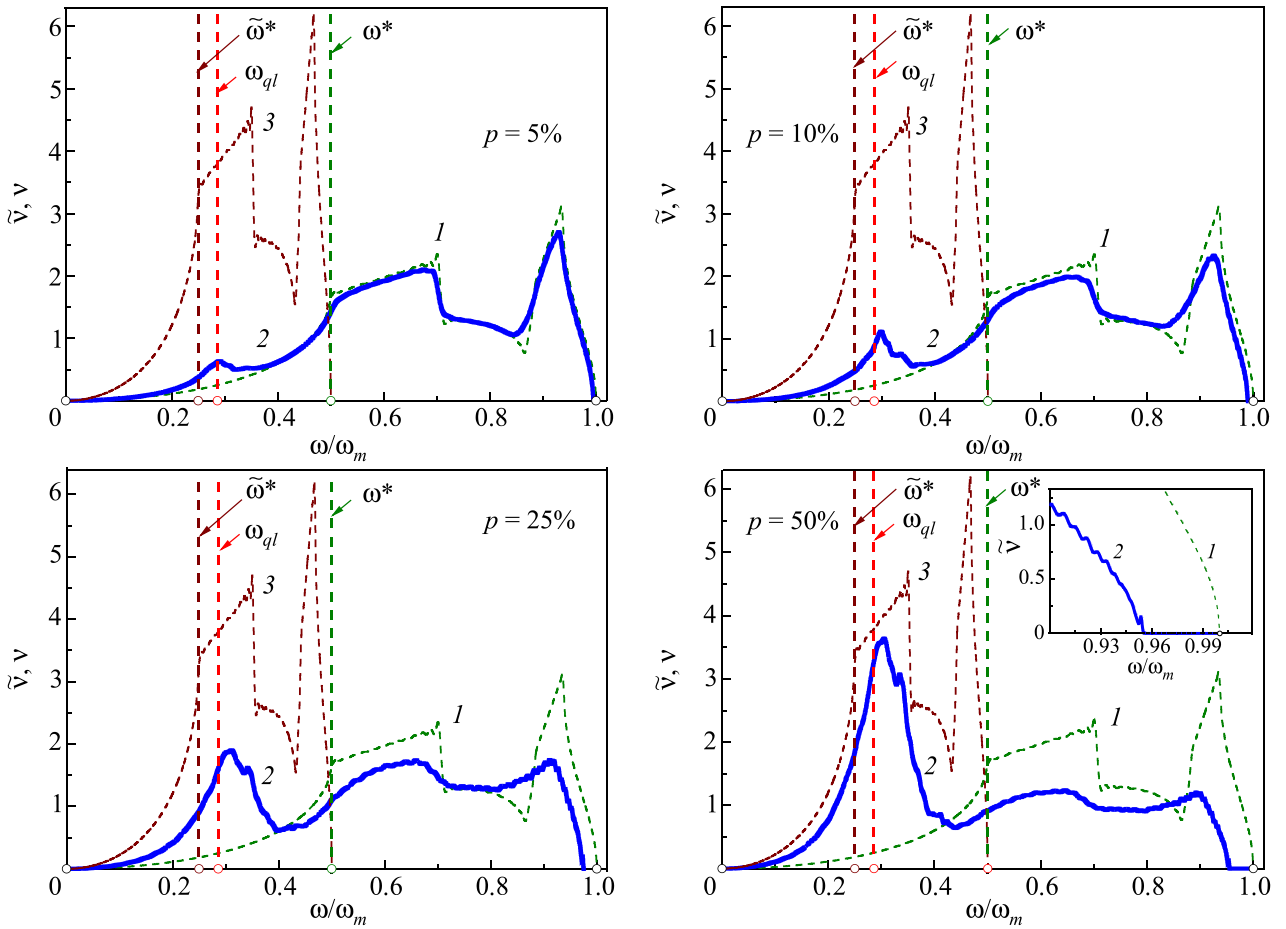

FIG. 4. The evolution of the phonon density of states of a disordered solid solution, with an increase in the concentration of a heavy isotropic impurity.

interval and the corresponding singularities will be ironed out.

Already at $p = 0.1$, the quasi-local peak has a certain structure that bears a remote resemblance to the phonon density of states of the FCC crystal, determined by using a small number of moments in the J-matrix of rank 3–5,[19] which is due to the formation of impurity clusters of a corresponding size. The left slope of the peak becomes parabolic, and the quasi-local frequency becomes the new boundary of the propagon zone. At the same time, it's already possible to identify the high-frequency main lattice van Hove singularities, on the phonon density. With increasing concentration, the size of the impurity clusters grows, and the boundary of the propagon zone becomes more distinct. At $p = 0.25$ this boundary already has a fracture, analogous to the first van Hove singularity in a regular crystal. At $p = 0.5$, the transformation of the quasi-local maximum into the spectrum of the lattice of heavy atoms, is substantially complete. Two boundaries are clearly visible: the first separates propagons from diffusions, and another, above which the phonons propagate very slowly (locon region). In this region, the form of the curve $\tilde{\nu}(\omega,p)$ is reminiscent of a fractal (similar to one obtained in Ref. 30 for a one dimensional solid solution). It is clearly seen (see inset in panel $p = 0.5$) that the spectrum ends with an exponential damping of vibrations, which is characteristic of disordered systems.[23,24] The fact that the maximum frequency of the spectra shown in Fig. 4 differs from the so-called *natural boundary* (in this case, the maximum frequency of the main lattice) is explained by the rank of the J-matrices calculated by us, being finite ($n = 76$), and not allowing for an arbitrarily large cluster of either the main lattice atoms, or impurity.

Thus, a condition for the existence of QLV in the propagon zone, is the existence of a solution to Eq. (16) in this frequency range. The frequency of the quasi-local vibrations is determined by the frequency of the maximum on the imaginary part of the local Green function for the impurity atom. The arrangement of the quasi-local vibrations occurs at very small velocities, and can be represented in the form of diverging waves. At finite concentrations of the impurity p, scattering of quasi-planar acoustic waves occurs on the latter diverging waves, and already at $p \sim 10\%$ the quasi-local frequency becomes the top boundary of the propagon region of the solution's phonon spectrum.

4. The interaction of acoustic phonons with the quasi-localized vibrations; van Hove singularities and boson peaks

We will now analyze in more detail, the connection between the phonon dispersion, and the van Hove singularity in the phonon spectrum of an ideal crystal, and similar phonon spectra properties with broken crystal regularity in terms of atomic arrangement. For any solid body (both crystal and those not possessing translational symmetry of atomic arrangement) there exists a low-frequency range, in which the phonon dispersion law is acoustic $\omega(\mathbf{k}) = s(\kappa)k$, (where k is the $\mathbf{k}$ wave vector modulus; $\kappa \equiv \mathbf{k}/k$ is the unit vector in the direction of wave propagation, and $s(\kappa)$ is the velocity of

sound as a function of direction). The phonon density of states in this range has the Debye form $\nu_D(\omega) = 3\omega^2/\omega_D^3$. Here $3\omega_D^{-3} = V_0 \sum_{i=1}^{3} s_i^{-3}/6\pi^2$, and values of s_i are obtained from the values of $s(\kappa)$ by averaging over all directions

$$s_i = \oint s(\kappa) do/4\pi.$$

With an increase in the value of k, the phonon dispersion law increasingly deviates away and down from the linear, and the real density of states deviates up and away from the Debye form.

Boson peaks as maxima along the relationship of $\nu(\omega)/\omega^2$, should only be examined for $\omega < \omega^*$, since a maximum along this relationship, corresponding to the first van Hove singularity ($\omega = \omega^*$), always exists. In the given frequency interval (propagon zone) the phonon density can be approximated by a certain parabola, and its deviation from the Debye density $\nu_D(\omega)$ can be expressed in terms of the frequency dependence on the value of ω_D, i.e., the phonon density can be written as

$$\nu(\omega) = \frac{3\omega^2}{\omega_D^3(\omega)}. \qquad (23)$$

Therefore, using the definition of ω_D (for example, see Ref. 34), the relationship of the phonon density to the square of the frequency, can be expressed through the dispersion of the sound velocities $s_i(\omega)$

$$\frac{\nu(\omega)}{\omega^2} \equiv \frac{3}{\omega_D^3(\omega)} = \frac{V_0}{6\pi^2} \sum_{i=1}^{3} s_i^{-3}(\omega),$$

where V_0 is the unit cell volume. Thus, the occurrence of the maximum along the $\nu(\omega)/\omega^2$ ratio, is due to the additional dispersion of sound velocities, caused by structural inhomogeneities, which are the source of quasi-local vibrations (defects, rotational degrees of freedom of the lattice nodes, etc.), and also the complicated structure of the unit cell.

In an ideal crystal, where the dependence $\omega(\mathbf{k})$ is a periodic function, and $\mathbf{k}$ is a quasi-wave vector for some value $k = k^*$, the group velocity of phonons of some transverse acoustic modes, for one of the crystallographic directions, vanishes. Typically, this direction coincides with the direction of one of the axes of symmetry in the $\mathbf{k}$-space, and the value of k^* corresponds to the boundary of the first Brillouin zone in this direction. Therefore, the transition from closed isofrequency surfaces to open, occurs at the frequency $\omega^* = \omega(k^*)$, and the value ω^* is the frequency of the first van Hove singularity (for the model examined in this study, the frequency of the FCC crystal lattice is $\omega^* = \omega_m/2$).

In Fig. 5(a), we see the density of states of the FCC crystal lattice, with central closest-neighbor interaction, and dependences on the frequency of the group velocities of longitudinal and transverse phonons, along highly symmetric crystallographic directions ΓX, ΓL and ΓX (one octant of the first Brillouin zone of the FCC crystal is shown on the right, for convenience). The Debye density of states $\nu_D(\omega) = 3\omega^2/\omega^3{}_D$, coincides sufficiently well with the true density of sates $\nu(\omega)$ at $\omega \leq 0.25\omega_m$. At $\omega \approx \omega_m/4$, the curve $\nu(\omega)$ starts to deviate upward from the $\nu_D(\omega)$ curve. The first van Hove singularity corresponds to the vanishing of the group

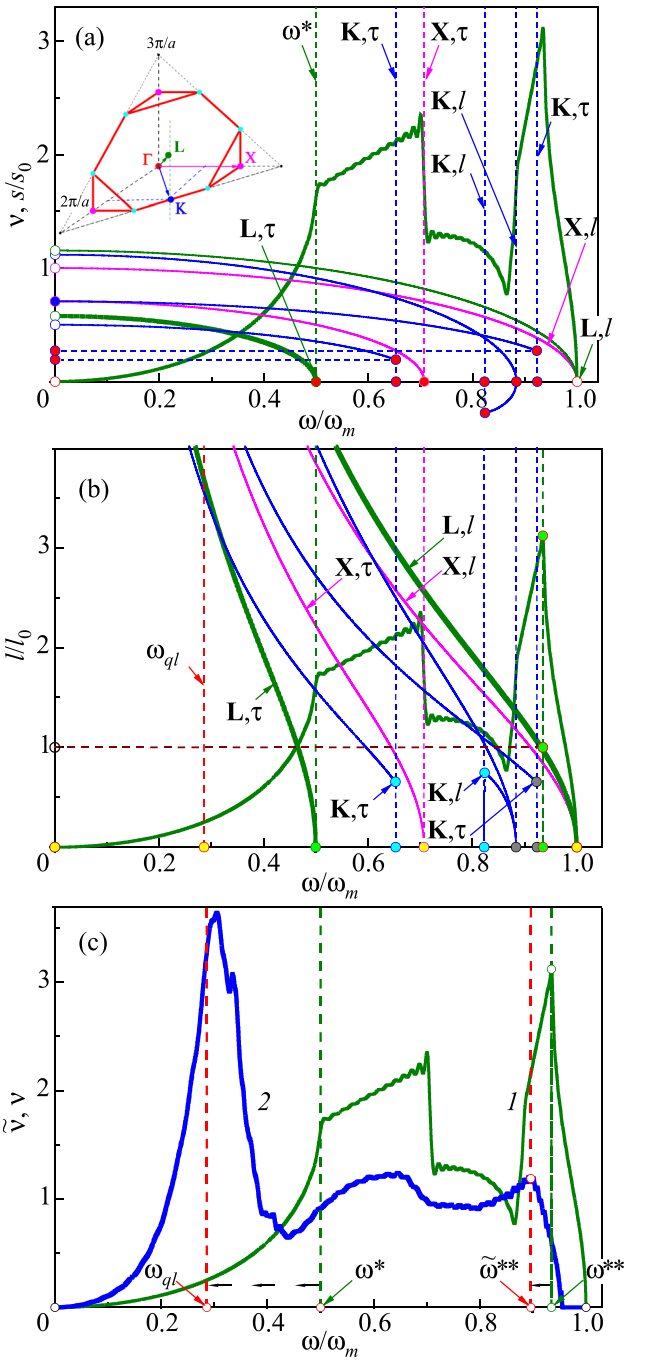

FIG. 5. Frequency dependence of group velocities (a) of the phonon mean free path over the oscillation period (b) and the classification of acoustic phonons in ordered and disordered structures (c). On (a) we see the first octant of the first Brillouin zone of the FCC crystal lattice, and designations of high-symmetry directions. The values: $s_0 = a\omega_m/4$; $l = 2\pi|s(\omega)/\omega|$; $l_0 = a/\sqrt{2}$.

velocity of transverse mode phonons, propagating along the direction ΓL (the given dependence is presented in the figure by the thicker line). At $\omega \geq \omega^*$ the character of the phonon dispersion changes significantly. Along with rapidly spreading phonons, the dispersion law of which still resembles the linear (the $s(\omega)$ dependence for other branches and propagation directions, as seen in the figure, at $\omega \approx \omega^*$ is relatively small), localized states appear, and transverse phonons no longer propagate along the direction ΓL. If for $\omega \leq \omega^*$, the average group velocity of phonons decreases smoothly as frequency increases, then at $\omega = \omega^*$ it decreases abruptly, and the spread of transverse-polarized phonons stops in eight

directions [±1, ±1, ±1]. We will note that the phonon dispersion law presented here, as a variable of the frequency of the velocity of their propagation $s_i(\omega)$, is more naturally generalized to disordered systems than the $\omega(\mathbf{k})$ dependence, as it contains no explicit dependence on the quasi-wave vector.

The frequency of the first van Hove singularity ω^*, is the interface between the fast and slow phonons, or propagons and diffusions, in an ideally ordered crystal. Using the terms from Ref. 14, it can be examined as an analogue of the Ioffe-Regel crossover in a regular crystal system. At $\omega = \omega^*$, the average wavelength is greater than the interatomic distance. Let us examine the distance that a phonon with the frequency ω, covers during its vibrational period $l(\omega) = 2\pi|s(\omega)|/\omega$. The frequency dependences $l(\omega)$ are presented in Fig. 5(b). Already at $p = 1\%$, the value $l(\omega)$ is greater than the average distance between impurity atoms, and at such concentrations of the impurity, the scattering of acoustic phonons on the quasi-local vibrations will have Ioffe-Regel properties, and express itself in the behavior of the spectral densities, in a form similar to the shape of the first van Hove singularity in an ideal crystal. We will also note that at ω^{**}, or the frequency of the highest-frequency van Hove singularity, which corresponds to the transfer from open to closed isofrequency surfaces, the value $l(\omega)$ for the longest wavelengths of vibration, or longitudinal oscillations propagating along the ΓL direction (isolated in the figure with a thick line), becomes equal to the distance between the closest neighbors, $l_0 = a/\sqrt{2}$. As in, for $\omega > \omega^{**}$, the phonons can be examined as quasi-local states. This frequency range has the name *locon zone*, and phonons with the frequency greater than ω^{**} are referred to as *locons* (for example, see Ref. 1).

In Fig. 5(c), we have the division of the frequency range into the propagon, diffusion, and locon regions, for the ideal FCC crystal, and a disordered solid solution of the type $A_{0.5}B_{0.5}$, the phonon density of which is shown in Fig. 4(d) (isotopic solution of atoms with mass ratio 1:4). As noted earlier, for an ordered crystal, the propagon zone (ΠΓ) corresponds to the frequency interval [0, ω^*]. In this interval, the phonon density of states has a parabolic (quasi-Debye form), which corresponds to the phonon propagation of all polarizations, along all crystallographic directions. For a disordered solid solution $A_{0.5}B_{0.5}$, the phonon density of states also has a quasi-Debye parabolic form, but in the interval [0, ω_{ql}]. As in, the propagon zone becomes more narrow. This almost free dispersion of phonons, at first glance, in a completely disordered solution, can be explained by the fact that for the lighter atoms of the solution at these frequencies, phonon dispersion is small. Practically, these are acoustic waves, which can be freely dispersed in completely disordered environments. In addition, since in our model the "crystal core" is totally preserved (all atoms are located at the nodes of the FCC crystal lattice, and only the atom type is random),then practically any solid solution can be presented as a certain ordered solution (more complex, than the initial) as long as there is a sufficiently small concentration of defects, such as "atomic transitions from one sublattice to another."

The frequency ω_{ql} is the top limit of the propagon zone of the solid solution ($\omega_{\text{pr–diff}}$), which is very noticeable with its increasing concentration. Let us examine the appearance of boson peaks and the Ioffe-Regel crossover in the phonon spectra of solid solutions. In Fig. 6 we see the evolution of the $\nu_{\text{imp}}(\omega)$ value with an increasing concentration of impurity; it is the contribution to the phonon density of states from displacements of the impurity atoms, in comparison to the values of $p\tilde{\rho}^{(\tau_-^5)}(\omega)$ (curves 3 and 4 on the left panels of the figure). We also see evolution of the $\tilde{\nu}(\omega) - \nu_{\text{imp}}(\omega)$ value, or the contribution due to the displacement of atoms in the main lattice, in comparison to the value $(1-p)\nu_{1n}(\omega)$ (curves 5 and 6 on the right panels) with increasing concentration. In all panels: curves 1 are the phonon density of states of the ideal main lattice; curves 2 are the phonon density of states of the solution.

The functions of $\nu_{\text{imp}}(\omega)$ differ from zero only in proximity to the maximum on curve $\tilde{\rho}^{(\tau_-^5)}(\omega)$ (frequency ω_{ql}). Therefore, the QLV can be presented as waves that are slowly diverging from the impurity, analogous to spheres. Curves 5 and 6 for high concentrations of impurity, have a typical ironed-out kink at $\omega \approx \omega_{ql}$, similar to the form of the first van Hove singularity. For frequencies smaller than ω_{ql}, the frequency dependences $\tilde{\nu}(\omega) - \nu_{\text{imp}}(\omega)$ have a typical parabolic shape, with little differentiation from the quadratic (Debye) form. The Debye behavior of the solution's phonon density inputs from the atoms of the main lattice at $\omega < \omega_{ql}$, is even more noticeable along the behavior of the frequency functions $[\tilde{\nu}(\omega) - \nu_{\text{imp}}(\omega)]/\omega^2$, which are shown on the magnified insets in the left panels of the figure. This confirms the earlier conclusion that at $\omega \leq \omega_{ql}$, the spread of atomic vibration of the main lattice is practically acoustic in character (they propagate in waves that are almost planar). The fractures along curves 2 and 5 correspond to the transition from fast spreading phonons (propagons) to slower (diffusions), due to the scattering on the QLV.

One could argue that even the ironed-out kinks at $\omega \approx \omega_{ql}$ on curves 2 and 5 in disordered solutions, and the first van Hove singularity in the ordered structures, have a common nature, such that they are both caused by an abrupt change in the average group velocity of phonons, and are manifestations of the Ioffe-Regel crossovers.

With further increase in the concentration of a solid solution, there is formation of impurity clusters that are sufficiently large, in which it is possible to identify different crystallographic directions. The frequency of the first van Hove singularity at $p = 100\%$ is $\tilde{\omega}^* < \omega_{ql}$, which corresponds to the vanishing group velocity of the transverse polarized phonons in the given clusters, along the crystallographic direction ΓL. The evolution of the low-frequency parts contributing to the phonon density of states from the impurity atoms, is shown in Fig. 7. The concentration p changes from 50% to 100%.

We will note that with an increase in the concentration of impurity atoms from $p = 0\%$ to $p = 50\%$, the disorder of the solution increases, which leads not only to a decrease in the width of the propagon zone, but also to a decrease in the "specific share" of the propagons in the phonon spectrum, i.e., the value

$$\int_0^{\omega_{\text{pr–diff}}} \tilde{\nu}(\omega)d\omega \approx \int_0^{\omega_{ql}} \tilde{\nu}(\omega)d\omega.$$

With continued increase of the impurity concentration, the solution can be examined as a solution with the

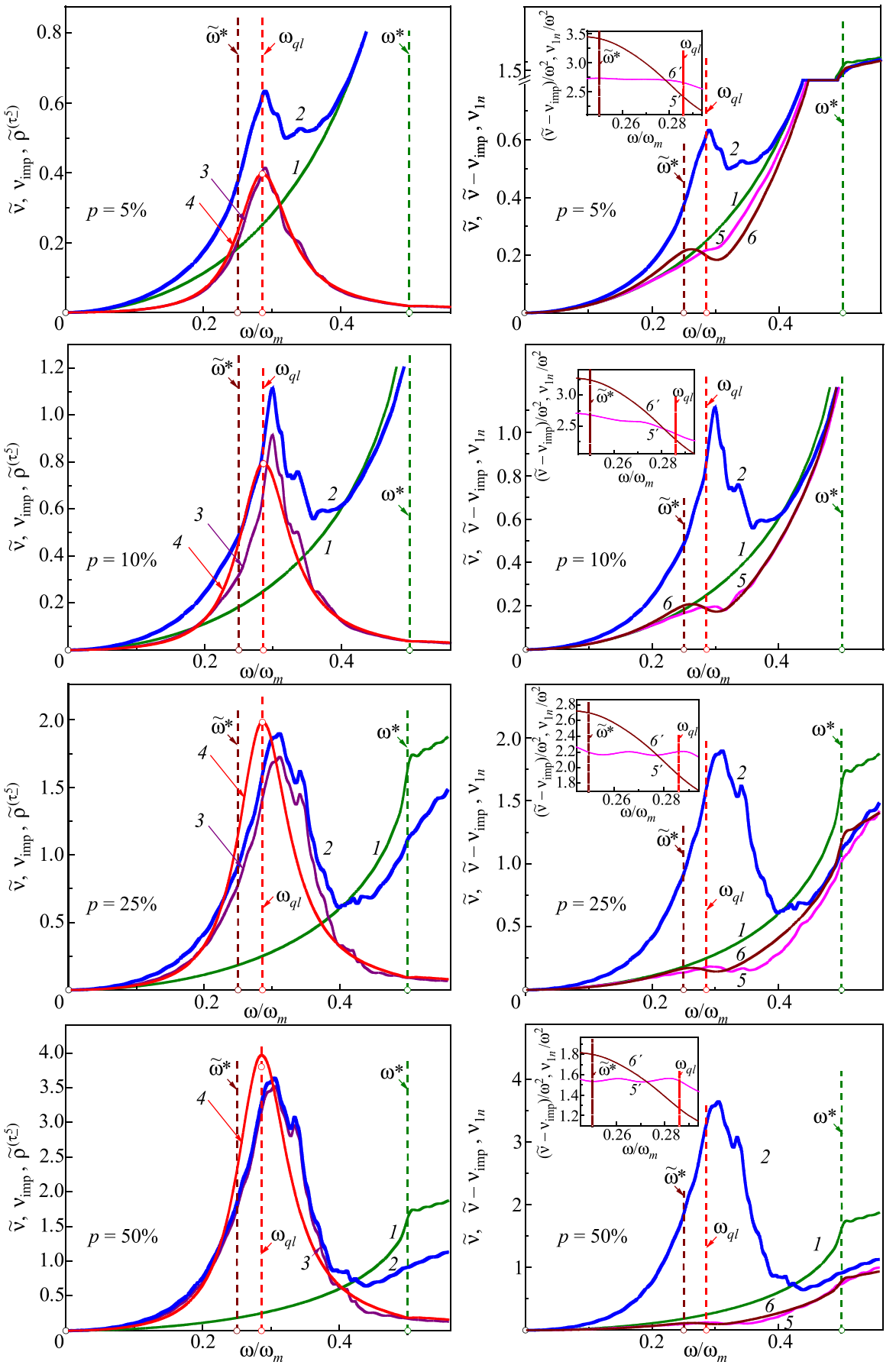

FIG. 6. Evolution of the contributions to the phonon density of states of a solid solution, from vibrations of impurity atoms (on the left) and vibrations of atoms of the main lattice (on the right), with an increasing impurity concentration.

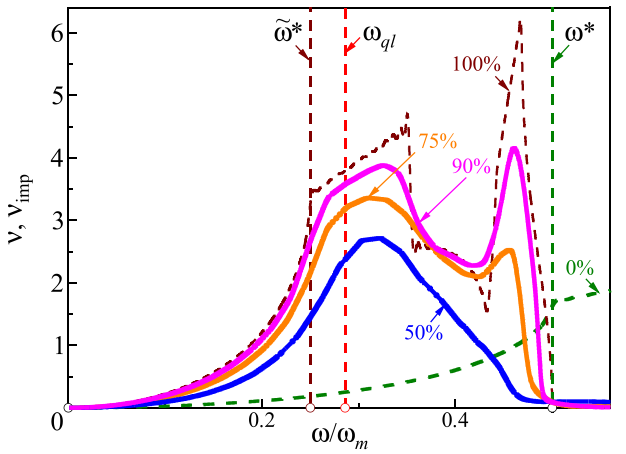

FIG. 7. The contribution of impurity atoms, to the low-frequency phonon density of states of solid solutions, with a high concentration of impurity.

concentration $1-p < 50\%$, with a light impurity in a heavy matrix, the degree of disorder of which decreases against an increase in p, which leads to an increase in the specific share of the propagons in the phonon spectrum. At $p = 100\%$, the lattice is completely ordered, and the specific share of the propagons in its phonon spectrum is the same as it is in the phonon spectrum of the initial crystal. It is obvious that the performed expression is

$$\int_0^{\omega^*} \nu(\omega)d\omega = \int_0^{\tilde{\omega}^*} \tilde{\nu}_{p=100\%}(\omega)d\omega.$$

As such, the influence of heavy atoms, or impurity atoms that are loosely coupled to the atoms of the main lattice, on the phonon spectrum and the vibrational properties, is manifested both in the formation of quasi-local vibrations, due to the natural oscillations of the impurities themselves, and in the scattering by these vibrations, of fast acoustic phonons that are generated by atomic oscillations of the main lattice.

5. Manifestation of quasi-local vibrations and boson peaks, in the behavior of low-temperature heat-capacity

Measurements of low-temperature heat capacity over a course of many years, are one of the most important sources of information about the behavior of low-frequency vibrational spectra of solids, thanks to its high accuracy, and also relative (in comparison to neutron diffraction studies of the phonon spectra), cheapness, and simplicity. In particular, due to various defects, the enrichment of the low-frequency region of the phonon spectrum, is noticeably visible due to the changes of the temperature dependence of the specific heat, under the influence of these defects. A textbook example of this influence is the formation of a sharp maximum along the relative change of the low-temperature heat capacity of a crystal, with the introduction of heavy impurities, or impurities that are loosely coupled to the atoms of the main lattice, when QVL are being formed in the phonon spectrum.[17,18,32] In these references, we consider the cases of small concentrations of impurity, when changes to the phonon spectrum by way of impurity, can be described in the linear concentration approximation (14). For the heat capacity of the crystal with an impurity concentration p, we can write down

$$\tilde{C}_V(T) \approx C_V(T) + p\Delta C_V(T), \tag{24}$$

Here, as was the case in (14), symbols with the tilde are for the perturbed system, and those without the tilde, are for the ideal; $\Delta C_V(T)$ is the change in the heat capacity of the crystal, upon introduction of one impurity atom. The sharp maximum along the $\Delta C_V(T)/C_V(T)$ curve in this case, is almost completely caused by the impurity vibrations.

This section is an analysis of the behavior of the low-temperature heat capacity, at large concentrations of impurities, when the linear concentration approximation is not justifiable. As the concentration of the impurity atoms increases, there is an increase in contribution to the changes of the low-temperature heat capacity, by the impurity-induced changes of the vibrational spectrum of the atoms of the main lattice, i.e., due to the scattering of fast acoustic phonons on the QLV, associated with the fluctuations of these atoms. This leads to a significant deviation of the low-temperature heat capacity from its Debye form. Manifestations of the contribution to the scattering of propagons on the QLV, is most clearly visible along the temperature dependence of the expression $C_V(T)/T^3$, and the temperature dependence of the Debye temperature. This dependence can be found from the transcendental equation

$$C_v(T) = C_D(T) \equiv 3R\left\{D\left(\frac{\Theta_D}{T}\right) - \frac{\Theta_D}{T}D'\left(\frac{\Theta_D}{T}\right)\right\}, \tag{25}$$

where

$$D(x) \equiv \frac{3}{x^3}\int_0^x \frac{z^3 dz}{e^z - 1}$$

is the Debye function, and the heat capacity $C_v(T)$ is determined experimentally, or through microscopic calculation via (for example, see Refs. 25 and 26)

$$C_v(T) = 3R\int_0^{\omega_m} \left(\frac{\hbar\omega}{2kT}\right)^2 \mathrm{sh}^{-2}\left(\frac{\hbar\omega}{2kT}\right)\nu(\omega)d\omega, \tag{26}$$

which expresses the vibrational heat capacity through the phonon density of states of the system $\nu(\omega)$.

Fig. 8, for solid solutions of differing concentrations of heavy isotopic substitution impurity in the FCC lattice, with a central interaction of the closest-neighbor, shows the following temperature dependences between: the relative change of the phonon heat capacity in the top panel; the relationship between heat capacity and the temperature cubed in the middle panel, and the Debye temperature in the lowest panel.

The relative change in the heat capacity (top panel) characterizes only the enrichment of the low-frequency region of the phonon spectrum, by the introduction of heavy impurity atoms into the crystal, which is characterized by the formation of a low-temperature maximum along the given curve. As can be seen in Fig. 6, the phonon density of states of a solid solution, have maxima at the frequency $\omega \approx \omega_{ql}$. With

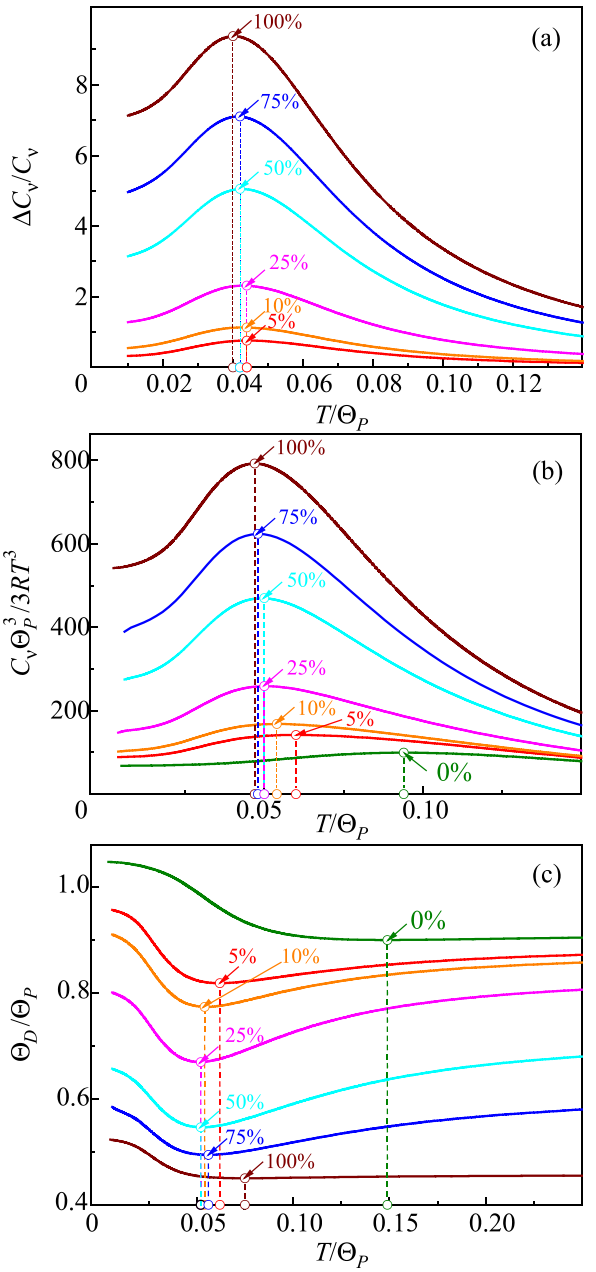

FIG. 8. Evolution with an increasing concentration of heavy impurity: relative changes in the heat capacity (a); the ratio of heat capacity to the cube of the temperature (b) and the temperature dependence of the Debye temperature (c).

an increasing concentration of impurity, the magnitude of this maximum grows in proportion to the magnitude of the concentration. Thus, there is a slow "pumping" of vibrational states from the frequency interval $\omega > \omega_{ql}$ into the frequency interval $\omega \leq \omega_{ql}$. As a result of this, the maximum of the relative change of heat capacity grows with the increase in the impurity concentration, and its temperature decreases slowly.

The maximum along the heat capacity/temperature cubed curve (middle panel), forms due to the divergence of the temperature dependence of heat capacity from its low-temperature limit. The given value characterizes not only the enrichment of the low-frequency region of the phonon spectrum, but, to some extent, the additional deviation of the phonon spectrum from the acoustic, as well as the phonon density of states from the quadratic Debye form, both caused by this enrichment. Therefore, as can be seen in the middle panel of Fig. 8, the temperature of the given maximum, with an increase in the concentration, decreases much faster, than the temperature maximum along the relative change of heat capacity. In a number of references (for example, see Ref. 16) the maximum along the $C(T)/T^3$ curve is directly identified with a boson peak.

More complete information about the deviation of the phonon spectrum from the Debye form, is contained in the temperature dependence of the Debye temperature, presented in the bottom panel of Fig. 8. Deviation of the phonon dispersion law from the acoustic, is caused by the discreteness of the crystal lattice (for example, see Ref. 33), and the scattering of the acoustic phonons by the quasi-localized states.[14,15] This deviation leads to a significant dependence of the value Θ_D on the temperature, particularly in the low-temperature region, and the formation of the $\Theta_D(T)$ function of the low-temperature minimum.[33,34] The temperature of this minimum, as shown in Ref. 34, is determined by the frequency of the first van Hove singularity, in which the inhibition of a number of acoustic phonons occurs (see Fig. 5(a)). The formation of a quasi-local maximum on the phonon density of states, which, as was shown in the previous section, is analogous to the one examined in Refs. 14 and 15, determines the deepening of the minimum along the $\Theta_D(T)$ curve, and the lowering of its temperature. With the increasing of concentration p, from 0% to 50%, the minimum deepens even more (against the background of the general lowering of the Debye temperature) and its temperature falls. At $p = 50\%$ the solution is the most disordered. At a continued increase in concentration, as noted in the previous section, the disorder of the solution decreases, and clusters of heavy atoms are formed, the size of which increases with the growth of p. Therefore, at further decreases in the Debye temperature, the minimum on its temperature dependence flattens out, and its temperature increases slightly to a value equal to the temperature minimum on the $\Theta_D(T)$ curve of the initial lattice, multiplied by the square root of the mass ratio (in our case, this is 1/2). The curves for $p = 0\%$ and 100% are similar $\Theta_D(T)_{p=0} = 2\Theta_D(2T)_{p=1}$.

6. Conclusion

This is a study of the common nature of van Hove singularities, Ioffe-Regel phonon crossovers, and boson peaks,* as anomalies of the phonon spectrum, occurring because of additional dispersions of group velocity fast-propagating phonons (propagons) on slow quasi-particles. Propagon, diffusion, and locon frequency intervals are defined for crystals and disordered solid solutions, and it is found that in ordered crystal structures, the role of the propagon-diffusion border is played by the first (and lowest-frequency) van Hove singularity. The formation of boson peaks during the scattering of acoustic phonons on quasi-local vibrations, in a disordered solid solution, is analyzed at a microscopic level. It is shown that in the propagon zone of the vibrational spectrum of disordered solid solutions, additional singularities, such as

*Reference 2 makes the assertion that there is experimental proof of the similarity between the nature of BP occurrence in glasses, and van Hove singularities in crystals.

fractures analogous to the first van Hove singularity, form along the phonon density of states, in ideal crystals.

The enrichment of the low-frequency region of the phonon spectrum is done not only by the formation of quasi-local states, but also by the decreasing rate of propagation of long-wavelength acoustic phonons, due to scattering by these same states. In order for the results of this slow-down to be clearly manifested in the form of maxima along ratio of the phonon density of states to the square of the frequency (boson peaks), or additional singularities such as Ioffe-Regel crossovers in the propagon zone, it is necessary to fulfill several conditions. First, the frequency of the scattering quasi-local states must be sufficiently low, such that the "power of the defect" would be large enough. Second, the size of the defect cluster must be sufficiently large (no less than twice the interatomic distance) for which a sufficiently high $p \sim$ 15%–20% concentration of defects is required. The second condition signals for the appearance of another parameter within the system, the length l, which is the mean free path of the phonon over the oscillation period, the value of which must exceed the interatomic distance. In our case, l plays the role of the *disordering parameter*. When the given conditions are fulfilled, as noted in Refs. 14 and 15, the continuum approximation becomes inapplicable even in describing the long-wavelength phonons.

We analyzed the influence of the formation of quasi-local vibrational states and their scattering of fast acoustic phonons, on the low-temperature heat capacity. We demonstrate a connection between the position of the propagon-diffusion border of the temperature, and the value of the maxima on the temperature curves of the relative change of heat capacity, and the relationship of the heat capacity to the temperature cubed, as well as to the increase in the temperature dependence of the Debye temperature.

We will note, that the quasi-local vibrations, on which the scattering of the fast acoustic phonons takes place, can be anharmonic (for example, see Ref. 16). However, as can be seen from the results of this study, which were obtained in a strictly harmonic approximation, the anharmonicity of the vibrations is not the cause of the boson peaks, or the deviation of the vibrational characteristics from the Debye form, or the appearance of the Θ_D temperature dependence.

The authors are grateful to K. A. Chishko for the fruitful discussion.

[a)]Email: gospodarev@ilt.kharkov.ua

[1]P. B. Allen, J. L. Feldman, J. Fabian, and F. Wooten, Philos. Mag. B **72**, 1715 (1999).
[2]A. I. Chumakov *et al*., Report on the 6th International Discussion Meeting on Relaxation in Complex Systems (New results, Directions and Opportunities), "Sapienza" Universita di Roma, Rome, Italy, August 30th–September 4th, 2009.
[3]F. Leonforte, A. Tanguy, J. P. Wittmer, and J.-L. Barrat, Phys. Rev. Lett. **97**, 055501 (2006).
[4]V. L. Gurevich, D. A. Parshin, and H. R. Schober, Phys. Rev. B **67**, 094203 (2003).
[5]B. Rufflé, M. Foret, E. Courtens, R. Vacher, and G. Monaco, Phys. Rev. Lett. **90**, 095502 (2003).
[6]L. Saviot, D. B. Murray, E. Duval, A. Mermet, S. Sirotkin, and M. C. Marco de Lucas, Europhys. Lett. **63**, 778 (2003).
[7]M. Arai, Y. Inamura, and T. Otomo, Philos. Mag. B **79**, 1733 (1999).
[8]B. Hehlen, E. Courtens, R. Vacher, A. Yamanaka, M. Kataoka, and K. Inoue, Phys. Rev. Lett. **84**, 5355 (2000).
[9]B. Rufflé, G. Guimbretière, E. Courtens, R. Vacher, and G. Monaco, Phys. Rev. Lett. **99**, 045502 (2006).
[10]V. Buchenau, N. Nücker, and A. J. Dianoux, Phys. Rev. Lett. **53**, 2316 (1984).
[11]N. Ahmad, K. W. Hutt, and W. A. Phillips, J. Phys. C: Solid State Phys. **19**, 3765 (1986).
[12]D. Engberg, A. Wischnewski, U. Buchenau, L. Börjesson, A. J. Dianoux, A. P. Sokolov, and L. M. Torell, Phys. Rev. B **59**, 4053 (1999).
[13]S. R. Elliott, Europhys. Lett. **19**, 201 (1992).
[14]M. I. Klinger and A. M. Kosevich, Phys. Lett. A **280**, 365 (2001).
[15]M. I. Klinger and A. M. Kosevich, Phys. Lett. A **295**, 311 (2002).
[16]M. A. Ramos, M. Hassaine, B. Kabtoul, R. J. Jiménez-Riobóo, I. M. Shmyt'ko, A. I. Krivchikov, I. V. Sharapova, and O. A. Korolyuk, Fiz. Nizk. Temp. **39**, 600 (2013) [Low Temp. Phys. **39**, 468 (2013)].
[17]Yu. Kagan and Ya. Iosilevskiy, J. Exp. Theor. Phys. **42**, 259 (1962); **44**, 284 (1963); **45**, 819 (1963).
[18]G. H. Panova and B. M Samoilov, J. Exp. Theor. Phys. **49**, 456 (1965).
[19]V. I. Peresada, "A new computational method in the theory of harmonic vibrations of the crystal lattice," Ph.D. dissertation phys-math, sci. (Kharkov, 1972).
[20]V. I. Peresada, in Coll. Condensed Matter Physics, ILTPE, Kharkov, 1968.
[21]V. I. Peresada, V. N. Afansyev, and V. S. Borovikov, Fiz. Nizk. Temp. **1**, 461 (1975) [Sov. J. Low Temp. Phys. **1**, 227 (1975)].
[22]R. Haydock, in *Solid State Physics*, edited by H. Ehrenreich, H. Ehrenreich, F. Seitz, and D. Turnbull (Academic Press, New York, 1980), Vol. 35, p. 129.
[23]I. M. Lifshitz, L. A. Pastur, and S. A. Gredeskul, *Introduction to the Theory of Disordered Systems* (Nauka, Moscow, 1982).
[24]I. M. Lifshitz, S. A. Gredeskul, and L. A. Pastur, *Introduction to the Theory of Disordered Systems* (Wiley, New York, 1988).
[25]A. M. Kossevich, *Crystal Lattice Theory* (Vishcha School, Kharkov, 1988).
[26]A. M. Kossevich, *The Crystal Lattice (Phonons, Solitons, Dislocations*) (WILEY-VCH Verlag Berlin GmBH, Berlin, 1999).
[27]I. M. Lifshitz, J. Exp. Theor. Phys. **17**, 1076 (1948).
[28]I. M. Lifshitz, Usp. Mat. Nauk **7**, 171 (1952).
[29]O. V. Kovalev, *Irreducible Representations of Space Groups* (Publishing House of the Academy of Sciences of the Ukrainian SSR, Kiev, 1961).
[30]M. A. Ivanov, Yu. V. Skripnik, and V. S. Molodits, Fiz. Nizk. Temp. **30**, 217 (2004) [Low Temp. Phys. **30**, 159 (2004)].
[31]L. D. Landau and E. M. Lifshitz, *Statistical Physics* (Nauka, Moscow, 1964).
[32]V. G. Manzheliy, V. P. Chausov, and S. I. Kovalenko, FTT **12**, 2764 (1970).
[33]G. Leibfrid, *Microscopic Theory of the Mechanical and Thermal Properties of Crystals* (Fizmatlit, Moscow-Leningrad, 1963).
[34]I. A. Gospodarev, V. I. Grishayev, A. V. Kotlyar, K. V. Kravchenko, E. V. Manzheliy, E. S. Syrkin, and S. B. Feodosyev, Fiz. Nizk. Temp. **34**, 829 (2008) [Low Temp. Phys. **34**, 655 (2008)].

Translated by A. Bronskaya